cmgh
CELLULAR AND MOLECULAR GASTROENTEROLOGY AND HEPATOLOGY

ORIGINAL RESEARCH

Growth Factor Independence-1 (*Gfi1*) Is Required for Pancreatic Acinar Unit Formation and Centroacinar Cell Differentiation

Xiaoling Qu,[1] Pia Nyeng,[1,2] Fan Xiao,[1,3] Jorge Dorantes,[1] and Jan Jensen[1]

[1]Cleveland Clinic, Department of Stem Cell Biology and Regenerative Medicine, Cleveland, Ohio; [2]Danish Stem Cell Center, University of Copenhagen, Copenhagen, Denmark; [3]Ottawa Hospital Research Institute, Ottawa, Ontario, Canada

SUMMARY

In a knockout mouse model, growth factor independence-1 (*Gfi-1*) plays an important role in regulating the development of pancreatic centroacinar cells and the formation and structure of the pancreatic acinar/centroacinar unit.

BACKGROUND & AIMS: The genetic specification of the compartmentalized pancreatic acinar/centroacinar unit is poorly understood. Growth factor independence-1 (*Gfi1*) is a zinc finger transcriptional repressor that regulates hematopoietic stem cell maintenance, pre-T-cell differentiation, formation of granulocytes, inner ear hair cells, and the development of secretory cell types in the intestine. As *GFI1*/*Gfi1* is expressed in human and rodent pancreas, we characterized the potential function of *Gfi1* in mouse pancreatic development.

METHODS: *Gfi1* knockout mice were analyzed at histological and molecular levels, including qRT-PCR, in situ hybridization, immunohistochemistry, and electron microscopy.

RESULTS: Loss of *Gfi1* impacted formation and structure of the pancreatic acinar/centroacinar unit. Histologic and ultrastructural analysis of *Gfi1*-null pancreas revealed specific defects at the level of pancreatic acinar cells as well as the centroacinar cells (CACs) in $Gfi1^{-/-}$ mice when compared with wild-type littermates. Pancreatic endocrine differentiation, islet architecture, and function were unaffected. Organ domain patterning and the formation of ductal cells occurred normally during the murine secondary transition (E13.5–E14.5) in the $Gfi1^{-/-}$ pancreas. However, at later gestational time points (E18.5), expression of cellular markers for CACs was substantially reduced in $Gfi1^{-/-}$ mice, corroborated by electron microscopy imaging of the acinar/centroacinar unit. The reduction in CACs was correlated with an exocrine organ defect. Postnatally, *Gfi1* deficiency resulted in severe pancreatic acinar dysplasia, including loss of granulation, autolytic vacuolation, and a proliferative and apoptotic response.

CONCLUSIONS: *Gfi1* plays an important role in regulating the development of pancreatic CACs and the function of pancreatic acinar cells. *(Cell Mol Gastroenterol Hepatol 2015;1:233–247; http://dx.doi.org/10.1016/j.jcmgh.2014.12.004)*

Keywords: Centroacinar Cells; Claudin 10; Growth Factor Independence-1 (*Gfi1*).

The digestive functions of the pancreas are provided by acinar cells. Structurally, glandular acini constitute the main mass of pancreatic parenchyma, organized within pancreatic lobuli. Acini are composed of pyramid-shaped cells that surround a centroacinar lumen. Drainage of digestive juice is initially performed by a small duct that is commonly referred to as the intercalated duct. The intercalated ducts invaginate the acini, and the distal-most cells of the intercalated ducts have been referred to as centroacinar cells (CACs). Electron microscopy has allowed for three-dimensional visualization of the acinar unit structure, revealing that intercalated duct-type cells are not obligatorily connected to the main ductal tree but may intersperse within the larger acinar structure.

Acinar cells secrete directly into the luminal portion at places lined with intercalated ductal cells. The developmental origin of intercalated ductal cells has not been established, but such are generally viewed as being thought to develop from the identical origin as that of the main ductal tree, which then would argue for an early developmental fate allocation presumably occurring at the time of ductal fate assignment in early embryogenesis.[1] A general absence of markers to distinguish between CACs and the intercalated duct cells of the pancreas has not allowed a clear separation of the two cell types, and studies investigating a possible differential, or identical, origin of such cells through lineage tracing has not been possible. Genetic components identifying the mechanism of CACs development have not been found.[2]

Production of low protein/high bicarbonate fluid by the intercalated ductal cells and CACs helps to solubilize acinar cell secretions, and the neutralizing effect of bicarbonate helps to normalize pH in duodenum after gastric emptying. Neutralization of pH locally may be important for neutralizing the content of exocrine secretory granules. Although mature exocrine granules are at neutral pH, immature granules are known to be acidified[3] through the activity of the vacuolar V-ATPase.[4] Such granule acidification is a requirement for the pathological intracellular activation of

Abbreviations used in this paper: **BPL, Bauhinia purpurea lectin; BrdU, bromodeoxyuridine; CACs, centroacinar cells; DIG, digoxigenin; EM, electron micrographs; *Gfi1*, growth factor independence-1; PBS, phosphate-buffered saline; qRT-PCR, quantitative real-time polymerase chain reaction; rER, rough endoplasmic reticulum; SD, standard deviation; TipPC, tip progenitor cells; TrPC, trunk progenitor cells; TUNEL, terminal deoxynucleotidyl transferase-mediated dUTP nick end labeling; WT, wild type.**

2352-345X
http://dx.doi.org/10.1016/j.jcmgh.2014.12.004

zymogens that occurs after supramaximal cholecystokinin or caerulein treatment,[5,6] which eventually leads to acinar cell death. The structural manifestation is one of intracellular, acidified vacuoles in which cathepsin B catalyzes the intracellular activation of zymogens. The insufficient neutralization of secretory juice is related to acinar disease. For example, intraductal acidosis is a manifestation of acute biliary pancreatitis.[5,7]

There is mounting evidence on the ontogeny of the major pancreatic cell fates through genetic lineage tracing, but knowledge of ductal cell-type specification in the pancreas is sparse.[2,8] The major ductal population of the pancreas has been shown to occur during a process referred to as organ domain patterning, which prefigures the secondary transition and helps segregate multipotent pancreatic progenitor cells into two distinct subsets, called trunk progenitor cells (TrPCs) and tip progenitor cells (TipPCs). Notch signaling is required for TrPC formation, and TipPC form upon Notch signaling abrogation.[9,10] Expression of specific transcription factors is spatially controlled during TrPC/TipPC formation, where *Hnf1β* (*Tcf2*), *Hnf6* (*Oc1*), and *Sox9* are expressed in the TrPC population, in contrast to *Ptf1a* which is expressed only by TipPC (as reviewed elsewhere[8,11,12]).

As *Hnf1β*, *Hnf6*, and *Sox9* remain expressed in ductal descendants of TrPC but are not expressed in endocrine descendants, these markers are useful for tracking ductal cell development. These factors are also expressed in CACs, which are also dependent on Notch signaling.[13–15] Therefore, it seems plausible that CACs are defined as a subpopulation of ductal descendants originating from the TrPC population. However, it also remains possible that TipPC acinar descendants could generate the CACs population, if such could reactivate Notch signaling, which subsequently could involve activation of the aforementioned intrinsic factors. The latter possibility is intriguing, considering multiple reports of acinar cell plasticity during adult organ regeneration, including reactivation of Notch signaling.

We have observed that *Gfi1* plays a role in the control of the functional acinar/centroacinar cell unit. *Gfi1* is critical during hematopoiesis and inner ear cell development, and it also plays a role in maintaining the functions of the lungs and intestines.[16–19] *Gfi1* is expressed during development in distalized pancreatic progenitors, corresponding to TipPC, and remains expressed in acinar descendants. The absence of *Gfi1* does not abrogate acinar differentiation, and a complement of all pancreatic lineages, including endocrine, duct, and acinar cells, develops normally. However, after differentiation of the exocrine pancreas of *Gfi1* nulls, acinar cells develop structural abnormalities in which they lose apical polarity. Electron microscopy analysis of *Gfi1*-null acinar cells has identified a general loss of rough endoplasmic reticulum (rER) associated with excessive cellular content of immature secretory granules. Postnatally, *Gfi1*-null exocrine cells become highly vacuolated. The exocrine phenotype is characterized by a particular reduction of CACs, as evidenced by an apparent elimination of the expression of several markers such as *Hnf6*, *Hnf1β*, and *Sox9* in the position of CACs. We conclude that *Gfi1* is required for the formation of CACs, and we believe *Gfi1* is the first factor in forming the genetic requirements for creating and maintaining the acinar/centroacinar structural unit.

Materials and Methods

Animals

The *Gfi1*$^{+/-}$ mouse line (*Gfi1*^{tm1sho}, MGI: 2449921) was provided by Dr. Stuart Orkin. This targeting model contains a deletion of exon 2–3.[20] Vaginal plugs were checked the next morning before 10:00 AM, and the time-mated embryos were dissected as described elsewhere.[21] The animals were housed in the animal facility at the Cleveland Clinic. All animal procedures and experiments were approved by the Cleveland Clinic Animal Care and Use Committee.

Histology and Immunofluorescence Analysis

Tissues were fixed in 4% paraformaldehyde at 4°C overnight, were washed in 1× phosphate-buffered saline (PBS), and were equilibrated in 30% sucrose before embedding in optimal cutting temperature compound, before the cryosectioning. The immunostaining protocol was followed as described elsewhere.[21] Antigen retrieval was performed with a neutral-pH antigen-retrieval agent.

The tissue samples were stained with the primary antibodies as detailed in Supplementary Table 1. For the anti-HNF6 antibodies staining, the Tyramide Signal Amplification Fluorescence system was used (PerkinElmer, Waltham, MA). Before applying the blocking reagents, the tissue samples underwent peroxidase (3% in PBS) treatment for 7 minutes. After incubating in the primary antibody (rabbit anti-HNF6) for overnight and being washed with PBS for 3 times (5 minutes/wash), the slides were incubated in biotinylated secondary antibody for 30 minutes at room temperature. After washing 3 times in 1×PBS (5 minutes/wash), the slides were further incubated in streptavidin-peroxidase conjugate for 15 minutes, which was then followed by three washes (5 minutes/wash). Then the slides were incubated in fluorophore tyramide (amplification reagent) for 3 to 10 minutes, which was followed by washing. Binding of the primary antibodies was detected by immunofluorescence by incubating with Texas Red-, Cy2-, or aminomethylcoumarin-conjugated secondary antibodies (Jackson ImmunoResearch Laboratories, West Grove, PA). After washing with 1×PBS, tissue samples were mounted (Slowfade Antifade kit; Molecular Probes/Life Technologies, Eugene, OR).

Immunohistochemical analysis for cell apoptosis was performed by using an in situ apoptosis detection kit with TUNEL (terminal deoxynucleotidyl transferase-mediated dUTP nick end labeling) according to the manufacturer's instructions (Roche, Indianapolis, IN). To evaluate the cell proliferation, we intraperitoneally injected mice with bromodeoxyuridine (BrdU) (50 μg/g of body weight). Two hours after the injection, the mice were dissected, and the pancreas were fixed and processed following the same protocol as previously mentioned for immunofluorescence analysis. Images were obtained using either an Olympus BX51 upright epifluorescence microscope (Olympus

America, Center Valley, PA), equipped with a QImaing Retiga 2000R cooled CCD camera (QImaging, Surrey, British Columbia, Canada) or a Leica SP5 confocal microscope (Leica Microsystems, Buffalo Grove, IL). Morphometry was done by measuring the number of positively stained cells per unit area using ImagePro 4.1 software image analysis system (Media Cybernetics, Rockville, MD).

In Situ Hybridization

The probe for the in situ hybridization analysis was generated by using the digoxigenin (DIG) labeling kit from Roche, according to the manufacturer's protocol. The probe was made from a linearized plasmid containing the *Gfi1* cDNA fragment (pCR-Gfi1) and T7 polymerase for antisense probes or T3 polymerase for sense probes by using the DIG RNA labeling mix (Roche). In situ hybridization was performed on frozen sections of 4% paraformaldehyde-fixed samples. After postfixation and protease treatment, sections were prehybridized at 65°C for 3 hours, followed by overnight hybridization with either antisense or sense probes at 65°C. The slides were then washed with 0.2×SSC/0.1% Tween 20 at 65°C for 1 hour. Sections then were blocked with 5% goat serum and 2% hybridization blocking reagent (Roche) for subsequent overnight incubation with an anti-DIG antibody conjugated with horseradish peroxidase at 4°C. After washing with 1×PBS/0.1% Tween 20, NBT (nitro-blue tetrazolium chloride)/BCIP (5-bromo-4-chloro-3′-indolyphosphate p-toluidine salt) (Roche) was used for signal detection.

Glucose Tolerance Test

Age- (10-week-old) and sex-matched wild-type (WT) (n = 4) and *Gfi1*-null mice (n = 3) were fasted for 16 hours. Before the test, the animals were weighed, and their preinjection blood glucose levels were measured. Filter-sterilized D-glucose (catalog no. G8270; Sigma-Aldrich, St. Louis, MO) was injected intraperitoneally (1 g/kg body weight), and blood was sampled at 0, 15, 30, 45, 60, 90, 120, and 150 minutes after the injection. The blood glucose level was measured with an Accu-Check Glucometer (Roche). The data are shown as the mean ± standard deviation (SD).

Electron Microscopy Analysis

Mouse pancreas (at the age of E18.5 and 1 month) (WT, n = 5; *Gfi1*-null, n = 4) were dissected, and small pieces were immediately fixed in 2% glutaraldehyde in 0.1 M sodium cacodylate buffer containing 0.1 M sucrose and 3 mM calcium chloride ($CaCl_2$) (pH 7.4) at room temperature for 4 to 8 hours, then stored at 4°C until further processing. Specimens were rinsed in 0.15 M sodium cacodylate buffer containing 3 mM $CaCl_2$ (pH 7.4), were postfixed in 2% osmium tetroxide in 0.07 M sodium cacodylate buffer containing 1.5 mM $CaCl_2$ (pH 7.4) at 4°C for 2 hours, were gradually dehydrated in ethanol, followed by acetone, and then were embedded in Epon resin. Semi-thin sections were cut and stained with toluidine blue and were used for light microscopic analysis. Ultrathin sections (40–50 nm) were cut and contrasted with 2% uranyl acetate followed by lead citrate. The ultrathin sections were examined on a Philips CS12/STEM transmission electron microscope (FEI Company, Hillsboro, OR) at Cleveland Clinic Lerner Research Institute Imaging Core. The total number of acini individually observed were 28 for WT and 20 for *Gfi1*-null.

Quantitative Real-Time Polymerase Chain Reaction

The embryonic and adult mouse pancreas at different developmental stages was isolated in RNAlater (Promega, Madison, WI). The total RNA were isolated and extracted by using RNAeasy RNA extraction kit following the manufacturer's manual (Qiagen, Valencia, CA). Total RNA extracted were reverse transcribed to cDNA using the SuperScript First-Strand Synthesis System based on the manufacturer's protocols (Invitrogen/Life Technologies, Carlsbad, CA). Quantitative real-time polymerase chain reaction (qRT-PCR) was performed with iQ SYBR Green Supermix (Bio-Rad Laboratories, Hercules, CA) according to the manufacturer's instructions and the protocols described elsewhere.[21] The expression levels of genes tested were normalized to the expression levels of the housekeeping gene *Gapdh* using the ΔΔCt method. Primer sets used were HNF1β (Tcf2), 5′-cca tcc tca aag agc tcc ag-3′, 5′-ctc cct ctg ggg gat att gt-3′; HNF6 (OC1), 5′-ctg tga aac tcc ccc agg ta-3′, 5′-ggt gat gat ggt gag gga ac; Sox9, 5′-tgc agc aca aga aag acc ac-3′, 5′-cag cgc ctt gaa gat agc at-3′; Ptf1a, 5′-cag agg acc cca gaa aac tca-3′, 5′-gtc aaa ggt gct tca gga aat c-3′; and Gapdh, 5′-tgc gac ttc aac agc aac tc-3′, 5′-atg tag gcc cat gag gtc cac-3′. The data are shown as mean ± SD.

Statistical Analysis

Statistical analyses were performed using the Student *t* test. $P \leq .05$ was considered statistically significant.

Results

Expression of Gfi1 in the Developing Mouse Pancreas

We first analyzed expression of *Gfi1* in the mouse pancreas at different developmental stages by performing qRT-PCR and in situ hybridization. From the mice embryonic stages of E12.5 to E16.5, *Gfi1* mRNA were present in pancreas (Figure 1*A*). At later stages of embryonic development (E17.5–E18.5) and the postnatal stage (P0 and P6), the *Gfi1* mRNA expression level was statistically significantly increased (Figure 1*A*). *Gfi1* was continuously expressed in the adult pancreas (1 month old and 4 months old, 1M and 4M).

To assess the cell-type specific expression of *Gfi1*, we performed in situ hybridization on developing mouse pancreas tissues (Figure 1*B*). At all stages analyzed, the pancreatic mesenchymal tissue was devoid of *Gfi1* expression, and the adjacent liver, containing hematopoietic cells, served as a useful positive control (Figure 1*B*).

Gfi1 was expressed in E11.5 pancreatic epithelium. At E14.5, when the pancreas progenitor population had segregated into the TrPC/TipPC regions, and acinar and

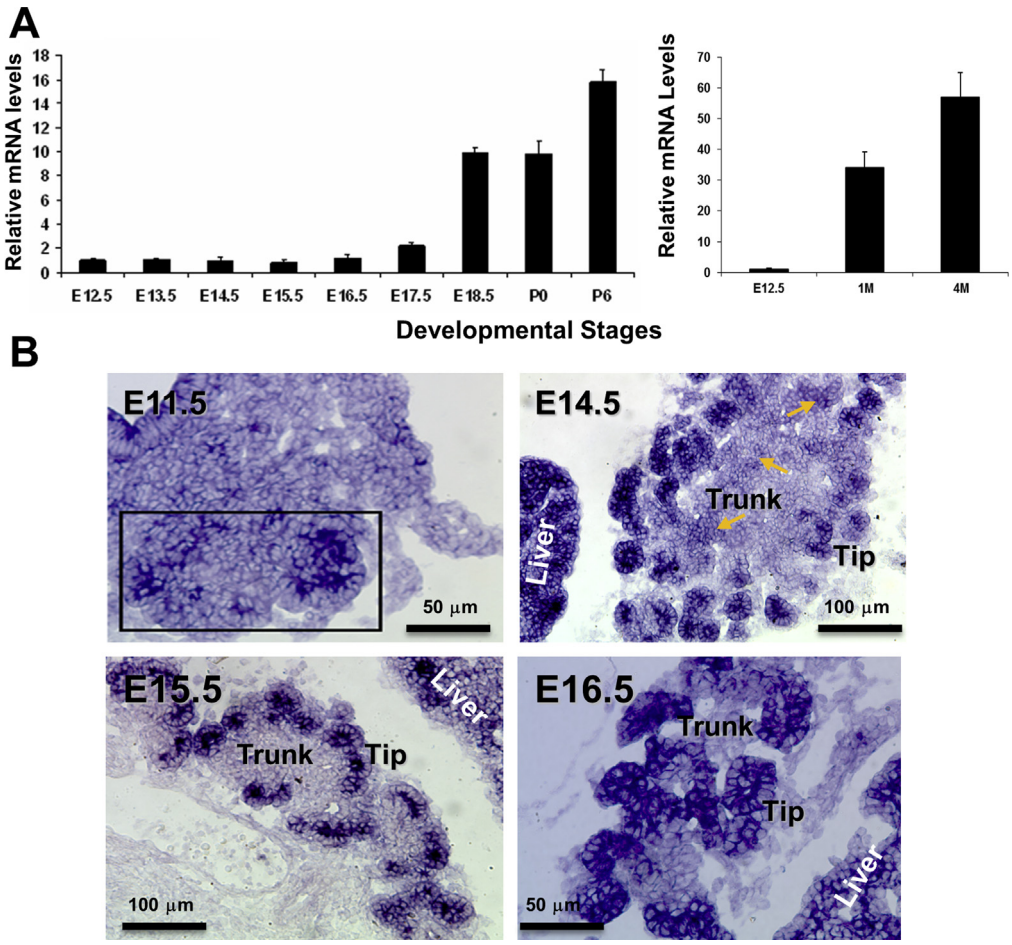

Figure 1. Expression profile of *Gfi1* in the developing and postnatal mouse pancreas. (*A*) Quantitative real-time polymerase chain reaction analysis of the expression pattern of *Gfi1* mRNA at the indicated developmental stages in the mouse: E12.5–E18.5 and postnatal (P0 and P6, and insert in showing 1 month old and 4 months old, 1M and 4M). Data shown (n = 3/time point) are mean ± standard deviation. (*B*) In situ hybridization analysis of the expression pattern of *Gfi1* mRNA in developing mouse pancreas (E11.5, 14.5, 15.5, and 16.5).

endocrine/ductal differentiation had commenced, *Gfi1* became restricted to "tip" regions, gradually being excluded from the central domain—the "trunk" regions—although the cells displaying intermediate levels of *Gfi1* mRNA could still be detected (arrows in Figure 1*B*, E14.5). At E15.5, *Gfi1* expression was fully excluded from trunk-located cells. At E16.5, *Gfi1* remained abundantly expressed in the cells at tips, and we observed a strict boundary between *Gfi1*-expressing cells at the tip location to adjacent epithelial *Gfi1*-negative cells (E16.5 in Figure 1*B*). The abundance of *Gfi1* mRNA in the post-secondary transition pancreas is suggestive of a functional role for *Gfi1* in pancreas development at the late developmental stages.

Acinar, but Not Endocrine, Defects in Gfi1*-Null Pancreas*

To functionally investigate *Gfi1* in pancreas, we bred for *Gfi1* nullizygous embryos and offspring using a global deletion model of exon 2–3 of *Gfi1*. Null animals suffer from severe neutropenia, loss of hearing, and a general growth deficiency.[16–19] Visual inspection of midgestational (E14.5), and late-gestational (E18.5) endodermal organs revealed a normal pancreatic size and gross appearance. Analysis of hematoxylin and eosin (H&E)-stained tissue at the embryonic stage of E14.5 and E18.5 did not reveal major changes in pancreatic morphology (Figure 2*A*–*D*). However, in adult mice (4 months old, 4M), morphologic changes were observed in the acinar compartment. The acinar architecture was poorly organized, marked by the presence of vacuolized structures within the acini (Figure 2*F*), when compared to the WT littermates (Figure 2*E*). At all stages studied, the pancreatic acinar morphology of *Gfi1* heterozygous mice was normal.

Considering that *Gfi1* is expressed during the secondary transition when endocrine cells form, we first investigated the development and function of pancreatic endocrine cells. The presence and organization of pancreatic endocrine cells were analyzed by immunofluorescence analysis against polypeptide hormones and chromogranin A. The presence of pancreatic endocrine cell types was confirmed by staining for insulin (β), glucagon (α), and ghrelin (ε) at E18.5. The endocrine cells' abundance and organization were comparable to WT mice. The central core of insulin-positive β-cells in the islets of Langerhans, surrounded by glucagon-positive α-cells, was observed in both the WT (Figure 2*I*) and $Gfi1^{-/-}$ pancreas (Figure 2*J*).

No difference in the expression of Pdx1 was observed in $Gfi1^{-/-}$ mice (Figure 2*H*). Pdx1 was confined to the nuclei of

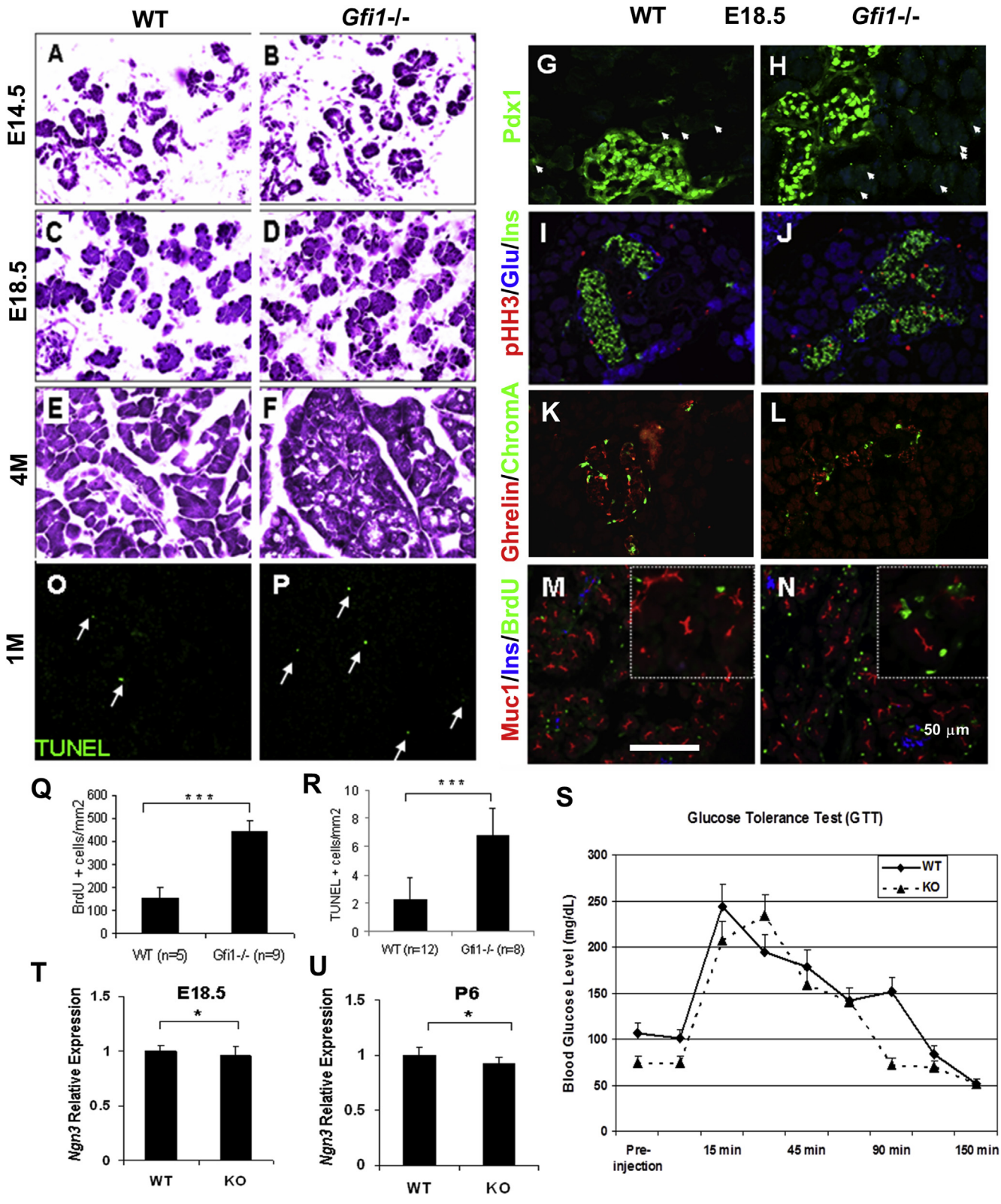

pancreatic insulin-producing cells at E18.5 (Figure 2*H*), as observed in WT littermates (Figure 2*G*), and was less abundantly expressed in acinar cells (arrows, Figure 2*G* and *H*).

Expression of ghrelin and the panendocrine marker chromogranin A (ChromA) were identified in *Gfi1*$^{-/-}$ mice (Figure 2*L*) as compared with WT mice (Figure 2*K*). We found no evidence of increased proliferation in the endocrine compartment at E18.5 using the M-phase marker pHH3 compared with WT (Figure 2*I* and *J*). Analysis of the E14.5 pancreas revealed a normal onset of pancreatic

endocrine cell differentiation at the secondary transition, with no apparent delay.

To assess adult β-cell function, we performed a glucose tolerance test in adult (10-week-old) *Gfi1*-null mice and WT littermates. The glucose clearing rate and fasting glycemic levels of the *Gfi1*-nulls remained comparable to the age-matched WT mice (Figure 2*S*). We have concluded that *Gfi1* is not essential for initiation of pancreatic endocrine cell differentiation, endocrine subtype fate assignment, the process of islet formation, or β-cell function.

The endocrine compartment remained normal, so we turned our investigation to the formation and structure of the acinar compartment. To more specifically define the onset of the acinar pancreatic phenotype, we first characterized the forming acinar compartment at E14.5. The initiation of acinar development can be visualized at E14.5 by the tip-cell expression of *Ptf1a* and the emergence of *Mist1*, which is expressed only in maturing acinar cells. Both these proteins were expressed at E14.5 in *Gfi1*-null mice (Figure 3*B* and *D*) in a pattern similar to WT littermates (Figure 3*A* and *C*). Using antibodies directed against carboxypeptidase A1 (CPA1) and amylase at E18.5, we found that the acinar compartment displayed similar immunoreactivity in the acinar cytoplasm between *Gfi1*-null and WT littermates. The acinar cells appeared to develop normally in the *Gfi1*-null mouse pancreas prenatally, but postnatally both CPA1 and amylase immunostaining revealed abnormal acinar units at the age of 1 month (1M) (Figure 3*F* and *H*) when compared with WT (Figure 3*E* and *G*). In addition, the typical pyramidal, wedgelike shape of individual acinar cells was lost in the *Gfi1*-null pancreas (Figure 3*F* and *H*). Furthermore, BrdU staining and TUNEL staining revealed increased cell proliferation (at E18.5) and cell apoptosis (at 1-month-old) in the *Gfi1*-null pancreas (Figure 2*N* and *P*) compared with WT littermates (Figure 2*M* and *O*), which was made further evident by quantitative analysis (Figure 2*Q* and *R*).

To better visualize the changes in the acinar/centroacinar units at the ultrastructural level, we performed transmission electronic microscopy analysis. Electron micrographs (EM) of WT pancreas showed the regular distribution of zymogen granules within the acinar cells (Figure 4*A* and *C*), a regular lumen with well-organized microvilli (Figure 4*D*), and the highly organized rER (Figure 4*E*). In contrast, EM of *Gfi1*-null pancreas revealed accumulated zymogen granules in the acinar units (Figure 4*B* and *F*) and autolysosomes (arrows in Figure 4*B*), a distorted lumen with disorganized microvilli (Figure 4*G*), and accumulation of cell secretions (arrows in Figure 4*G*). We noted a highly disorganized, excessively dilated rER in *Gfi1*-null pancreas (Figure 4*H*). Furthermore, EM revealed significant disturbance to the apical region of almost all acini in the *Gfi1*-null pancreas. This was evident by the irregular apical surfaces, indentations between individual exocrine cells, and vacuoles (Figure 4*F*). The latter likely resulted from intracellular activation of zymogens. The ultrastructural analysis also revealed the presence of CAC in WT (highlighted with a dotted line in Figure 5*A*), surrounded by zymogen-rich acinar cells, with which they share a lumen. In contrast to the WT pancreas, we noted that cells of a CAC morphology (small, cytoplasm sparse) and location (adjacent to the exocrine apical surface) were difficult to detect within the *Gfi1*-null pancreas (Figure 5*B*).

Gfi1 *Is Required for Centroacinar Cell Formation in Pancreas*

To further investigate whether CACs were affected in *Gfi1*-null mice, we performed an immunohistochemical analysis to localize and characterize these cell types, covering a larger field than provided by EM imaging. We chose to stain the pancreatic tissues by using fluorescently labeled Bauhinia purpurea lectin (BPL), a specific lectin that we have found only labels the acinar lumen. BPL displays little to no reactivity against pancreatic ductal cells. At E18.5, when the acinar units are maturing, BPL reactivity is highly restricted to the emerging acinar lumen (Figure 5*C*); an increase in BPL reactivity is noted as the organ matures (1M, Figure 5*E*). The BPL reactivity was completely absent in the E18.5 *Gfi1*-null pancreas (Figure 5*D*). BPL reactivity was disorganized and was observed with the distorted

Figure 2. (*See previous page*). Characterization of the *Gfi1*-null pancreas. (*A–F*) H&E staining of wild-type (WT) and *Gfi1*-null pancreas. At the embryonic stage of 14.5 and 18.5 (E14.5 and E18.5), there were no major changes in pancreatic morphology in *Gfi1*-null mice (*B, D*). However, at the age of 4 months (4M), morphologic changes were observed in the acinar compartment (*F*). The acinar architecture was poorly organized and marked by the presence of vacuolized structures within the acini (*F*) when compared with WT (*E*). (*G–N*) Immunohistochemical analysis of WT and *Gfi1*-null pancreas. The endocrine cells develop normally in the *Gfi1*-null pancreas (*H, J, L, N*), compared with WT littermates (*G, I, K, M*) at the embryonic stage of 18.5. In the *Gfi1*-null pancreas, Pdx1 was confined to the nuclei of pancreatic insulin-producing cells at E18.5 (*H*) as observed in wild-type (WT) littermates (*G*) and in both WT and *Gfi1* knockout pancreas less abundantly expressed in acinar cells (*arrows* in *G* and *H*). (*O, P*) Analysis of cell apoptosis by TUNEL staining. In the *Gfi1*-null pancreas, increased apoptotic cells were observed (*P*) compared with WT littermates (*O*). (*Q, R*) Morphometric quantification of the cell proliferation and cell apoptosis rate of WT and *Gfi1*-null pancreas. WT (n = 5) and *Gfi1*-null (n = 9) pancreas (E18.5) were analyzed for proliferation by bromodeoxyuridine (BrdU) injection, immunostaining for BrdU+ cells, and quantitative analysis (*Q*). WT (n = 12) and *Gfi1*-null (n = 8) pancreas (1 month old) were analyzed for cell apoptosis via TUNEL staining and followed by quantitative analysis (*R*). Graphs values are mean ± standard deviation (SD). ***$P < .001$. Scale bar: 50 μm. (*S*) Glucose tolerance test (GTT) was conducted in fasted adult (10-week-old) wild-type (WT) (n = 4) and *Gfi1*-null mice (n = 3). Fasting glycemic levels and the glucose clearing rate at various time points (15, 45, 90, and 150 minutes) of *Gfi1*-nulls remained comparable to age-matched WT mice. Graph values are mean ± SD. (*T, U*) Quantitative real-time polymerase chain reaction analysis of the expression pattern of *Ngn3* mRNA at the indicated developmental stages (E18.5 and P6) in WT and *Gfi1*-null pancreas. *$P < .01$.

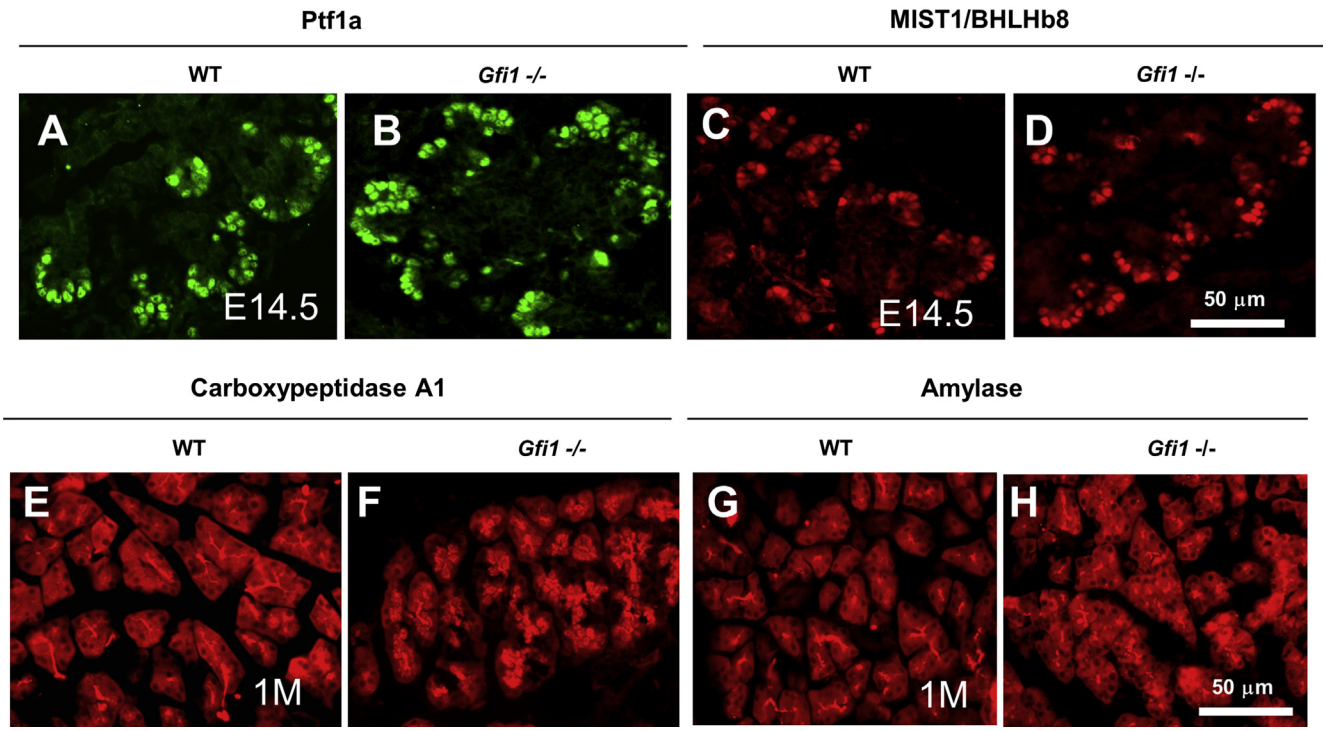

Figure 3. Exocrine defects in *Gfi1*-null mice. (*A–D*) Immunohistochemical analysis of Ptf1a (*A, B*) and MIST1 (*C, D*) expression in WT and *Gfi1*-null pancreas. Immunostaining using antibodies directed against Ptf1a and MIST1 protein shows that both of these proteins were expressed at E14.5 in *Gfi1*-null mice (*B, D*) in a pattern similar to WT littermates (*A, C*). (*E–H*) Immunohistochemical analysis of the other exocrine cell markers carboxypeptidase A1 (CPA1) and amylase in WT and *Gfi1*-null pancreas. Both CPA1 and amylase immunostaining revealed abnormal acinar units at the age of 1 month (1M) (*F, H*) when compared with WT (*E, G*). Scale bar: 50 μm.

acinar units in the 1-month-old *Gfi1*-null pancreas (Figure 5*F*), reflecting the EM morphology.

We also used antibodies directed against Claudin10 and Mucin1 (Muc1) to detect the morphology of acinar apical membranes. Claudin10 is highly specific for the cells in the CAC position (Figure 5*G*). This pattern in the pancreas reflects the presence of Claudin10 in terminal tubules in the murine submandibular gland.[22] Claudin10 immunoreactivity was lost in the *Gfi1*-null pancreas at E18.5 (Figure 5*H*). At the postnatal stage (6 days after birth, P6), specific defects were further observed at the level of pancreatic CACs in *Gfi1*-null mice when compared with WT littermates (Figure 5*O* and *P*). In the WT pancreas, Claudin10 protein specifically localizes at the apical membranes of acinar cells (arrows in Figure 5*O*), where the duct cells including *Sox9*+ CACs (arrowheads, Figure 5*O*) interconnect with acinar cells. However, in *Gfi1*-null mice, Claudin10 expression at the apical membranes of acinar cells dramatically decreased (arrows in Figure 5*P*), and *Sox9*+ CACs were rarely found (arrowheads in Figure 5*P*).

To examine the topology of ductal structures in the pancreatic tissues of *Gfi1*-null mice, we performed immunofluorescent staining with antibodies directed against Mucin1 (Muc1), a membrane protein expressed in the epithelial cells lining glands and ducts in multiple organs.[23] In the E18.5 WT pancreas, Mucin1 antibodies labeled all cells of the ductal system, including intercalated ducts and CACs, showing the well-structured branching of the ductal system and the radiations of small luminal areas (Figure 5*I*). *Gfi1*-null pancreas contained intercalated ductal cells but showed a lack of the terminal, radiating, branching structures as observed in WT (Figure 5*J*). The phenotype was more pronounced at 1 month of age (1M) (Figure 5*L*) compared with WT littermates (Figure 5*K*). Progression and worsening of acinar structural defects continued over time; at 4 months old (4M), the Mucin1-positive areas outlined the extensive vacuoles observed in the *Gfi1*-null pancreas (Figure 5*N*) compared with WT (Figure 5*M*).

Gfi1 *Deficiency Results in Acinar Degeneration and Regeneration after Birth*

We surmised that the ongoing deterioration of acinar function might be paralleled by a compensatory regenerative program. When compared with the WT (Figure 2*O*), we found a prevalence of apoptotic cells (TUNEL-positive staining) restricted to the pancreatic acinar compartment in the *Gfi1*-null pancreas (Figure 2*P*). Correspondingly, there was also an acinar-compartment-specific increased fraction of cells in the S-phase, as detected by short-term BrdU labeling (Figure 2*N*). Such a significant regenerative response would suggest substantial adaptive responses from one or more cell types in the pancreas, which could include dedifferentiation and redifferentiation events of existing

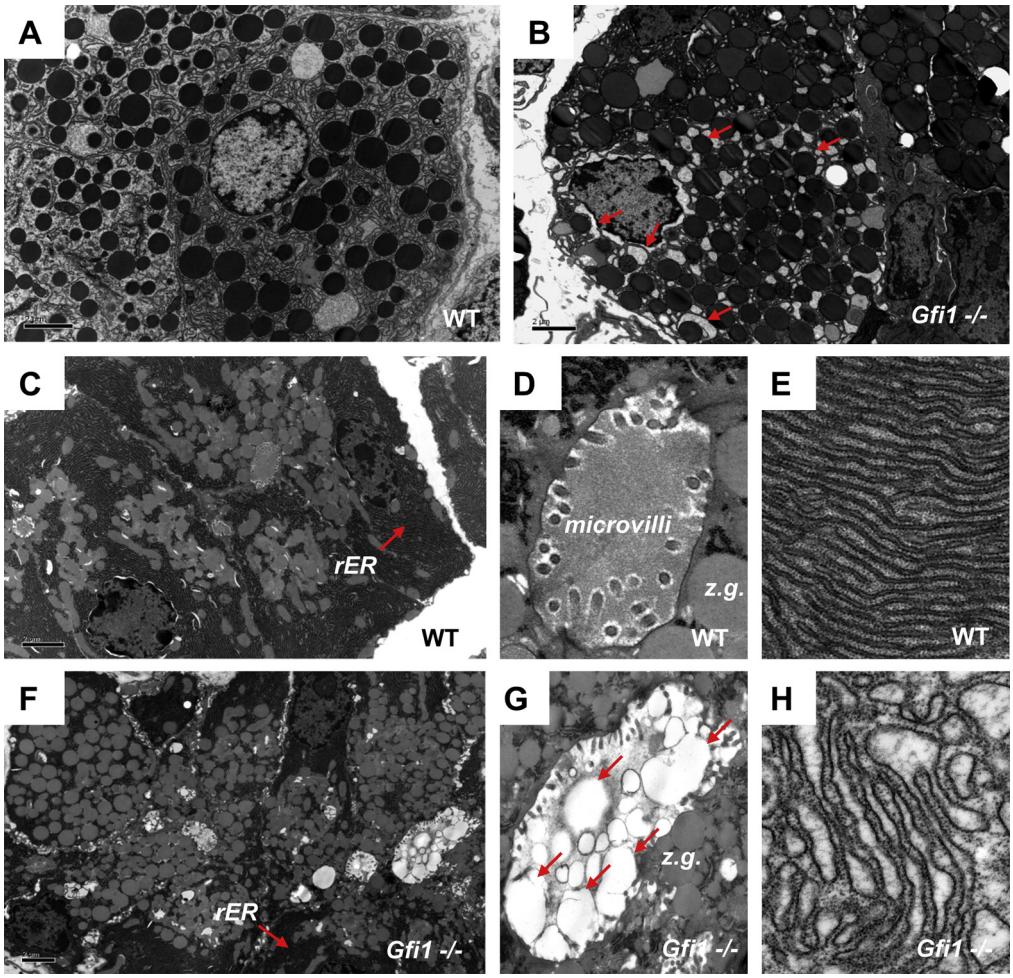

Figure 4. Ultrastructural changes of acinar cells in *Gfi1*-null mice. (*A–H*) Transmission electronic microscopy analysis of WT and *Gfi1*-null pancreas. The electron micrograph of the WT pancreas shows the regular distribution of normal zymogen granules in the acinar units (*A*, *C*), a regular lumen with well-organized microvilli (*D*), and a highly organized rough endoplasmic reticulum (rER) (*C*, *E*). However, the electron micrograph of *Gfi1*-null pancreas shows the extensively accumulated zymogen granules in the acinar units (*B*, *F*) and a distorted lumen with disorganized microvilli (*G*). In addition, the accumulation of cell secretions (*red arrows* in *G*) were noted, combined with highly disorganized, dilated rER (*F*, *H*).

cells (facultative replenishment) as seen after chemical injury,[24,25] or alternatively could involve the activation of genetic programs normally only observed during embryogenesis, such as *Ngn3* reactivation.[26] Expression of *Ngn3* mRNA was not found to be increased at E18.5 or postnatally (P6) in the *Gfi1*-null pancreas when compared with WT littermates via qRT-PCR analysis (Figure 2*T* and *U*), arguing against the reactivation of endocrine progenitor cells. It is possible that *Gfi1* would be required for facultative replenishment on a continuous basis, explaining the inability of the organ to recover; however, it is also possible that the initial effect of *Gfi1* loss led to a defective pancreatic structure from which regeneration was not possible, regardless of the status of *Gfi1*. Further investigations into this matter would demand an ability to perform a postnatal rescue of *Gfi1*.

Organ Domain Patterning and Ductal Cell Differentiation Is Normal in Gfi1*-Null Pancreas, but Formation of Centroacinar Cells in Late Gestation Is Impaired*

The developmental origin of CACs is currently unresolved but has been speculated to be ductal, occurring from *Sox9*-expressing cells.[27] Ductal cell differentiation is initiated at the secondary transition in mice (E13.5–E14.5), resulting from bipotential TrPC-type progenitors segregating into endocrine and ductal cells. The *Gfi1*-null pancreas displayed a normal distribution and amount of HNF1β- and Sox9-expressing cells at E14.5 (Figure 6*B*, *D*, *F*, and *H*) when compared with the WT littermates (Figure 6*A*, *C*, *E*, *G*). Such cells coexpressed the ductal marker Dolichos biflorus agglutinin (DBA) (Figure 6F and *H*), confirming their ductal identity. The HNF1β- and Sox9-expressing cells comprised the entire forming ductal system and extended to the forming acinar units (Figure 6*B*, *D*, *F*, and *H*), comparable to the WT pancreas (Figure 6*A*, *C*, *E*, and *G*). We conclude that the *Gfi1*-null pancreas initiated ductal development appropriately, and that the organ underwent an intact process of organ domain patterning between E11.5 and E13.5.

At E16.5, after completion of the secondary transition, a normal complement of HNF1β+, Sox9+, DBA+ cells was observed, extending throughout the ductal system (Figure 6*J*, *L*, *N*, and *P*) compared with the WT pancreas (Figure 6*I*, *K*, *M*, and *O*). However, at E18.5, HNF6+, Sox9+, and HNF1β+ cells, proximal to acinar units and thus corresponding to a centroacinar location, were reduced in the *Gfi1*-null pancreas

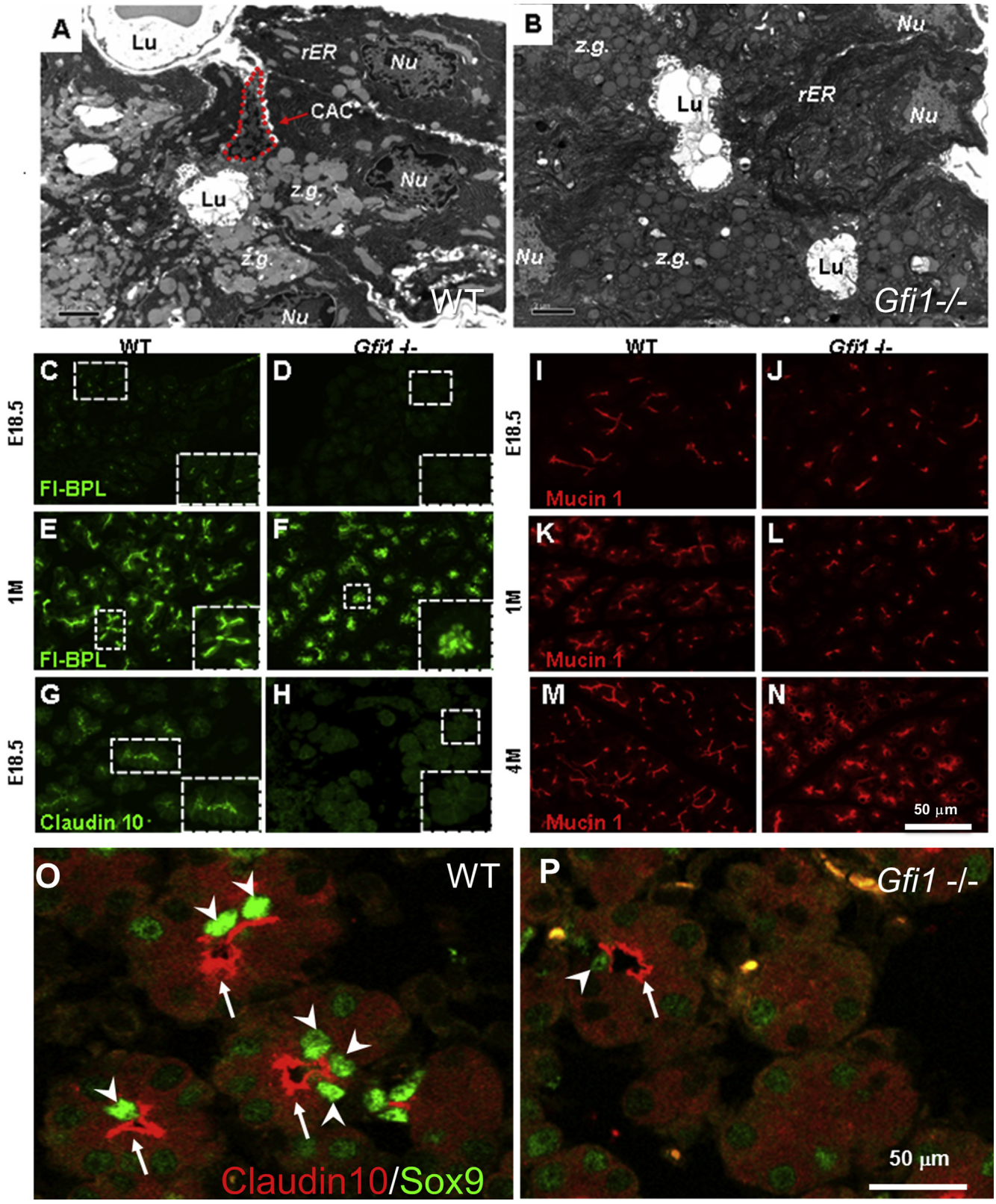

(Figure 7*B*, *B*′, *D*, *D*′, *F*, and *F*′) but were easily identifiable in the WT pancreas based on their expression, spatial location, and the typical centroacinar morphology of being cytoplasm sparse and containing flattened nuclei (Figure 7*A*, *A*′, *C*, *C*′, *E*, and *E*′). Over time, the reduction of HNF6-, HNF1β-, and Sox9-expressing CACs remained, and only few such cells

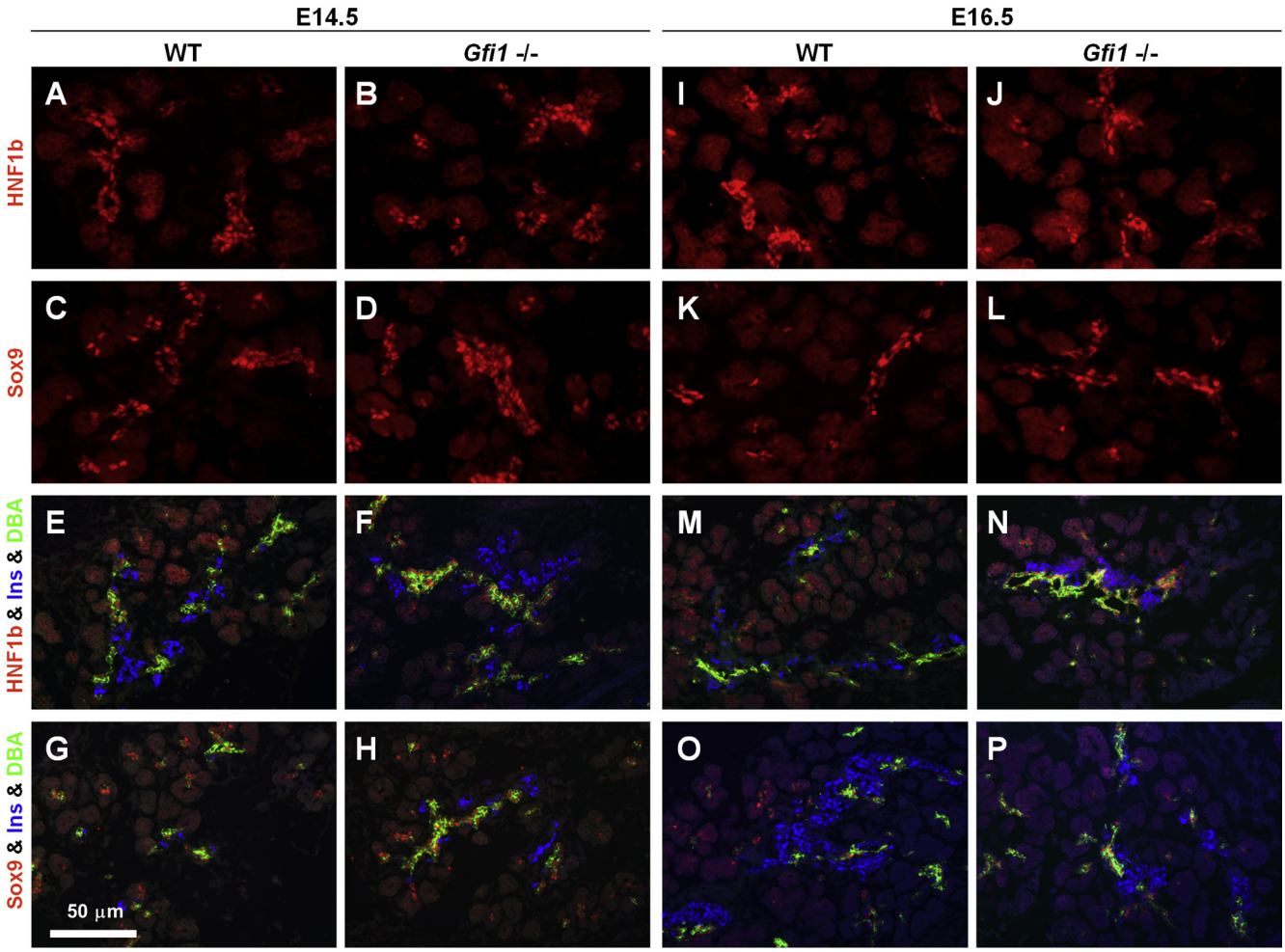

Figure 6. The pancreatic transcription factors *HNF1β*, *Sox9*, and *HNF6* are normally expressed in *Gfi1*-null pancreas at the stage of pancreatic secondary transition. (*A–H*) At E14.5, immunofluorescence analysis revealed that the expression of the pancreatic transcription factors *HNF1β*, *Sox9*, and *HNF6* in *Gfi1*-null pancreas (*B, D, F, H*) was unchanged compared with WT mice (A, C, E, G). (*I–P*) At E16.5, the expression pattern of the pancreatic transcription factors *HNF1β*, *Sox9*, and *HNF6* in the *Gfi1*-null pancreas (*J, L, N, P*) was comparable to that observed in WT mice (*I, K, M, O*).

could be detected at the age of 1 month (Figure 8*B, B′, D, D′, F,* and *F′*) when compared with the WT littermates (Figure 8*A, A′, C, C′, E,* and *E′*).

The reduced expression of these transcriptional factors in *Gfi1*-null mice was further confirmed by qRT-PCR for the mRNA levels of these genes (Figure 7*G*). Interestingly, the

Figure 5. (*See previous page*). Deficiency of centroacinar cells (CACs) in *Gfi1*-null pancreas. (*A, B*) Electron micrographs of WT and *Gfi1*-null pancreas. In the WT pancreas, a single CAC (*red dotted line*) is surrounded by zymogen (z.g.)-rich acinar cells, with which they share a lumen (Lu) (*A*). In contrast to the WT pancreas, in the *Gfi1*-null pancreas the structure consisting of CACs immediately adjacent to the exocrine apical surface was defective (*B*). (*C–F*) Immunohistochemical analysis of Bauhenia purpurea lectin (BPL). BPL reactivity was completely absent in the E18.5 *Gfi1*-null pancreas (*D*) compared with WT (*C*). BPL reactivity was disorganized and observed with the distorted acinar units in the 1-month-old (1M) *Gfi1*-null pancreas (F). (*G, H*) Immunohistochemical analysis of Claudin10. The staining of Claudin10 was diminished at the apical membrane of pancreatic exocrine cells in *Gfi1*-nulls (*H*) when compared with WT (*G*). (*I–N*) Immunohistochemical analysis of Mucin1 (Muc1). In the E18.5 WT pancreas, Mucin1 antibodies labeled all cells of the ductal system, including intercalated ducts and CACs, showing the well-structured branching of the ductal system and the radiations of small luminal areas (*I*). The *Gfi1*-null pancreas contained intercalated ductal cells but showed a lack of the terminal, radiating, branching structures observed in WT (*J*). The phenotype was more pronounced at 1 month old (1M) (*L*) compared with WT littermates (*K*). Progression and worsening of acinar structural defects continued over time; at 4 months old (4M), Muc1-positive areas outline the extensive vacuoles observed in the *Gfi1*-null pancreas (*N*) compared with WT (*M*). (*O, P*) At the postnatal stage (6 days after birth, P6), immunochemical analysis of Claudin10 and Sox9 demonstrates the defects in acinar apical membranes and CACs in *Gfi1*-null mice. In the WT pancreas, Claudin10 protein (*arrows*) specifically localizes at the apical membranes of acinar cells, where the duct cells including *Sox9*+ CACs (*arrowheads*) interconnect with acinar cells (*O*). However, in *Gfi1*-null mice, Claudin10 expression at apical membranes of acinar cells (*arrows*) dramatically decreased, and *Sox9*+ CACs (*arrowheads*) were rarely found (*P*). Scale bar: 50 μm.

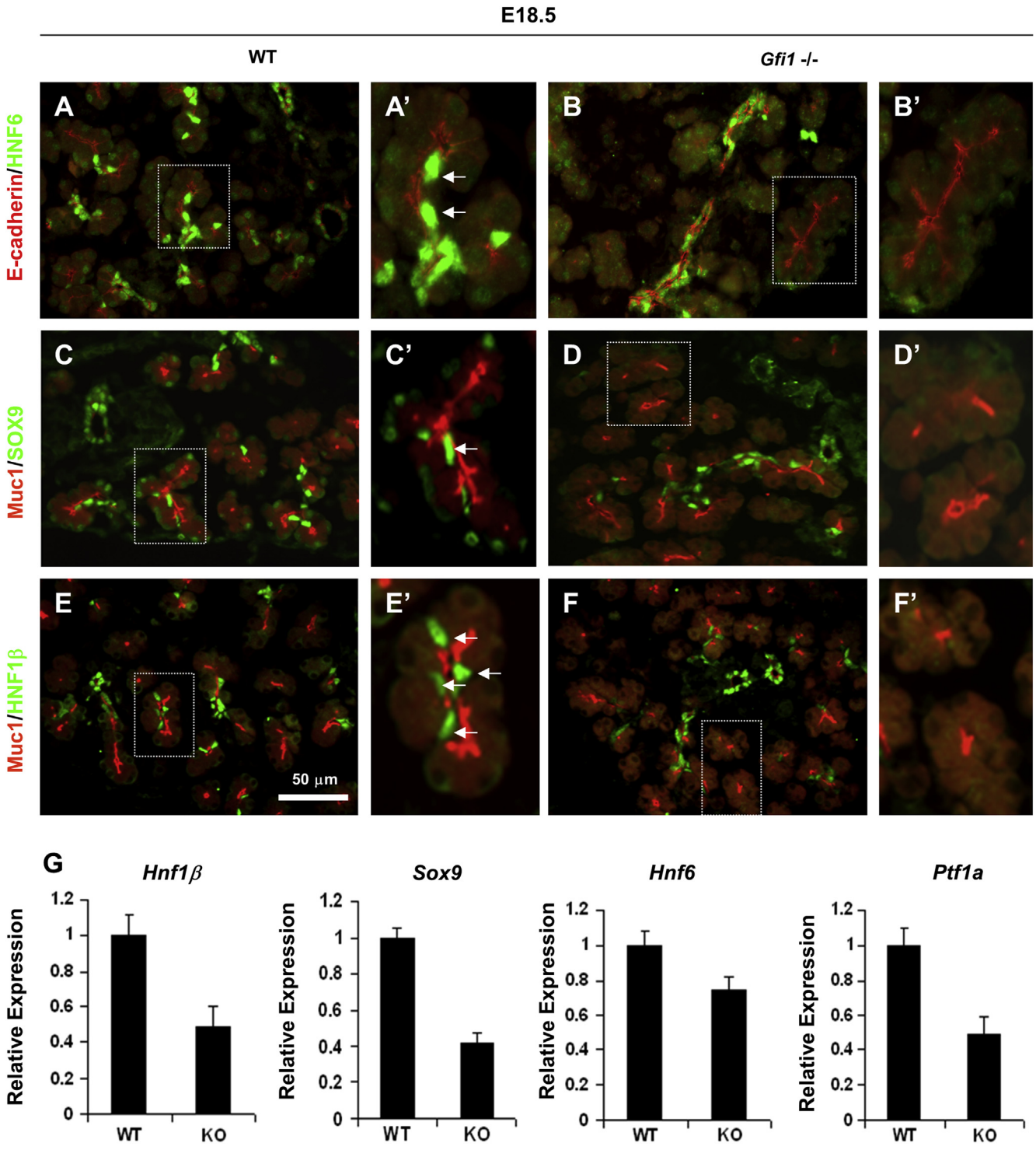

Figure 7. Loss of expression of centroacinar cell (CAC) regulatory factors in the E18.5 *Gfi1*-null pancreas. (*A–F′*) Immunofluorescence analysis of the CAC regulatory factors *HNF6*, *Sox9*, and *HNF1β*. At E18.5, *HNF6*+, *Sox9*+, and *HNF1β*+ cells, proximal to acinar units, thus corresponding to a centroacinar location, were reduced in the *Gfi1*-null pancreas (*B, B′, D, D′, F, F′*) but were easily identifiable in the WT pancreas based on their marker expression, spatial location, and the typical centroacinar morphology of being cytoplasm sparse and containing flattened nuclei (*A, A′, C, C′, E, E′*). Scale bar: 50 μm. (*G*) Reduced expression of the pancreatic transcriptional factors (*Hnf1b*, *Sox9*, *Hnf6*, and *Ptf1a*) in the *Gfi1*-null pancreas was identified by quantitative real-time polymerase chain reaction. Graph values are mean ± standard deviation.

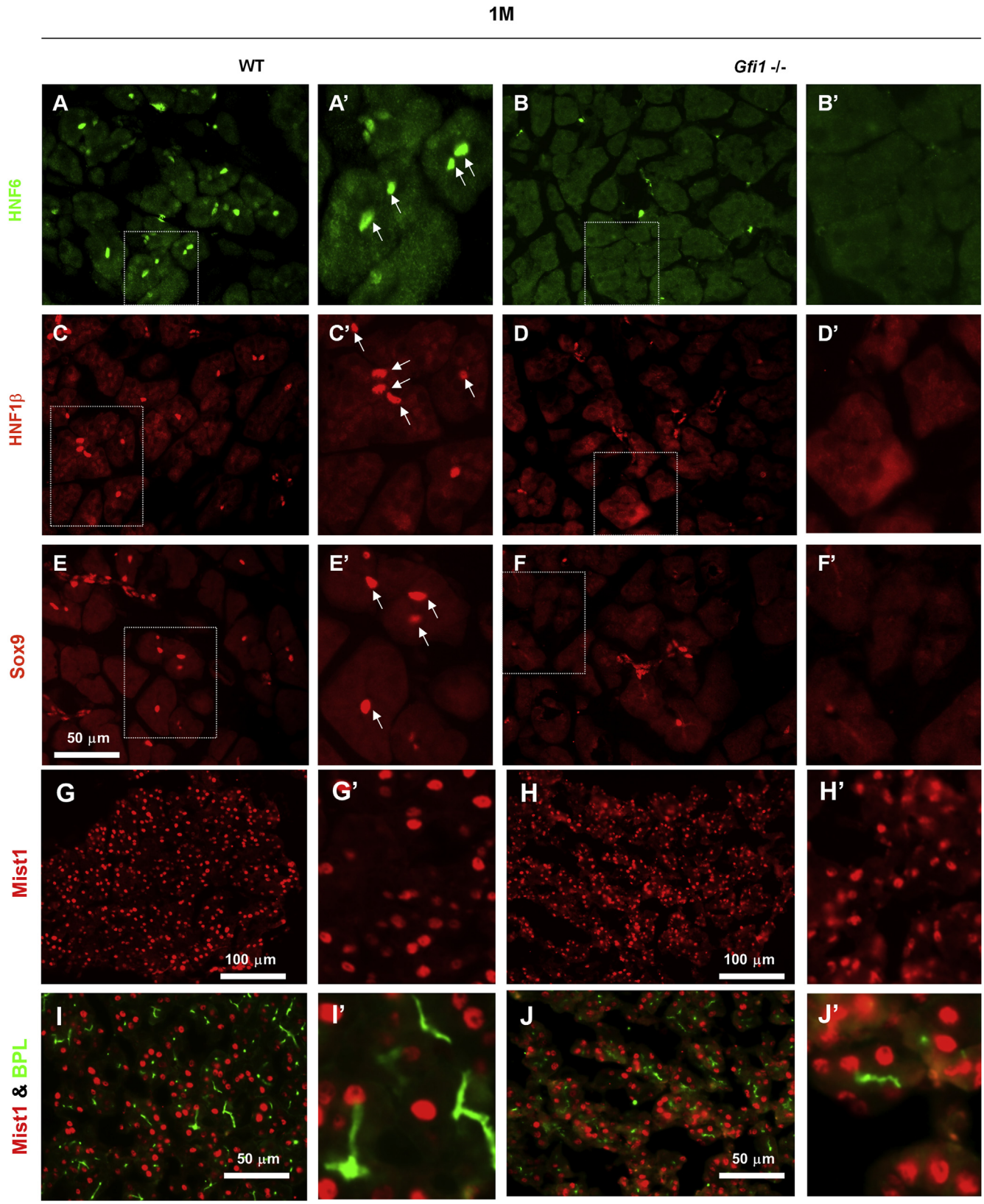

expression of the acinar/progenitor expressed gene *Ptf1a* was similarly reduced (Figure 7*G*), yet expression of the acinar terminal marker gene *bHLHb8*, encoding MIST1, remained expressed at normal levels and was detectable throughout the acinar cells in the *Gfi1*-null pancreas. The MIST1 protein expression pattern in the *Gfi1*-null pancreas

at 1 month old (1M) (Figure 8*H*, *H′*, *J*, and *J′*) did not appear to be noticeably different when compared with WT littermates (Figure 8*G*, *G′*, *I*, and *I′*). These data suggest that the *Gfi1*-null pancreas fails to establish a CAC population and that this process occurs between E16.5 and E18.5 in mice. This time period correlates very well with the significant increase in *Gfi1* gene expression between E17.5 and E18.5 (Figure 1*A*) in mouse development.

Discussion

Here, we report that *Gfi1* plays a role in late gestational development of the mouse pancreas. The *Gfi1*-null pancreas develops a specific phenotype related to the exocrine organ. The phenotype manifests between E16.5 and E18.5 and is correlated with a significant activation of *Gfi1* mRNA abundance. The main hallmark of the pancreatic response to a lack of *Gfi1* is the apparent lack of the distal-most ductal cell type in the organ, typically referred to as the CAC. Our data reveal a general disturbance to the organization of the acinar unit, impacting acinar cell polarity and resulting in a specific deficiency reflected by ultrastructural changes including internal vacuolization, expanded rER, and a particular deficiency in the organization of the apical cellular region.

The apical side of the acinar cell is normally connected to the intercalated ductal network, allowing for effective drainage of zymogens. We suggest that retention of zymogens in the acinar cells, the dilation of the acinar rER, and the loss of Claudin10 apical expression are secondary to the structural defects resulting from a lack of CACs, although an intrinsic role of *Gfi1* in the acinar cell cannot be ruled out. The apical deficiency of the acinar unit is significant as it appears to involve a gradual loss of HNF1β-, HNF6-, and Sox9-expressing cells at the very tip of the ductal network. However, the majority of the pancreatic ducts appear unaffected by a lack of *Gfi1*, and importantly both the development of the ductal lineage and the formation of a ductal tree structure, which occurs well before E18.5, are normal.

How *Gfi1* functions in the proper development of the interface between the ductal tree and the acinar cells of the pancreas is still unclear. Expression of *Gfi1* ranges from the hematopoietic and lymphoid system to the sensory epithelia such as inner ear hair cells as well as in Purkinje cells, lung and intestinal epithelial cells, and parts of the central nervous system.[17–20] Gene knockout studies have shown that loss of *Gfi1* affects pre-T-cell differentiation, the development of granulocytes, the development and function of dendritic cells, the development pulmonary of neuroendocrine cells, the integrity of inner ear hair cells, and the proliferation, differentiation, specification, and self-renewal of hematopoietic stem cells.[17–20] In the gut, *Gfi1* serves as a prodifferentiation factor that regulates the secretory versus endocrine fate switch.[18]

Except for the demonstrated role of *Gfi1* in the maintenance of hematopoietic stem cells, most studies implicate a specific role for *Gfi1* in cell fate determination. Considering that the pancreatic regulatory program shares multiple determinants with that of the gut, it is tempting to speculate that *Gfi1* may operate also in the pancreas for the determination of cell fate, here specifically related to the generation of CACs. The pancreas is, similar to the gut, composed of secretory and endocrine components. Considering that *Gfi1* in the gut plays a specific role opposed to Neurog3 (*Ngn3*) in facilitating the development of goblet and Paneth cells,[18] a possibility is that in the pancreas *Gfi1* is involved in differentiating a unique secretory cell type, the CACs, from the ductal compartment at a late stage (E17.5–E18.5).

At this point, our data are insufficient to prove which role *Gfi1* plays in CAC differentiation. It is currently unclear whether the lineage origin of the CACs is ductal or acinar, and experimental clarification would require lineage tracing from either compartment into the CACs, preferably under conditions in the absence or presence of the *Gfi1* gene function. Because of the known plasticity of the acinar cell compartment in adult pancreatic regeneration, CACs might descend from acinar cells. Although we used multiple commercial and published[18] antibody reagents to GFI1, these attempts failed to provide convincing data on the cell-type or spatial expression of GFI1 protein at the time of CAC differentiation.

Of note, *Gfi1* mRNA expression data determined by in situ hybridization revealed a tip-cell (ie, acinar-fated) expression of *Gfi1* in early pancreatic development (Figure 1*B*). It is thus possible that a subpopulation of already specified acinar cells commit to a CAC fate via the expression of *Gfi1*. Because multiple markers, such as HNF6, HNF1β, and Sox9, are commonly expressed between ductal cells and CACs, we hypothesize that *Gfi1* expression operates to segregate the distal-most ductal cells into specific CACs, and that in absence of *Gfi1* such specification fails. However, it is also possible that existing acinar cells begin to express the complement of these genes upon a CAC conversion. Further study is needed to distinguish between these two possibilities.

It is intriguing to speculate that *Gfi1* may be related to the maintenance of Notch signaling in the CACs, as it was previously shown that conditional deletion of *Rbpj* in the pancreas led to conversion of CACs into acinar cells.[14] Importantly, *Gfi1* has been shown to be required for the ability of immature hematopoietic cells to competently integrate Notch signaling.[28]

Figure 8. (***See previous page***). **Loss of expression of centroacinar cell (CAC) regulatory factors in the adult *Gfi1*-null pancreas.** (*A–F′*) Immunofluorescence analysis of *HNF6*, *HNF1*β, and *Sox9* reveals reduced or absent expression of these transcriptional factors at the position of the CACs in the *Gfi1*-null pancreas at the age of 1 month (1M) (*B*, *B′*, *D*, *D′*, *F*, *F′*) comparing with the WT pancreas (*A*, *A′*, *C*, *C′*, *E*, *E′*). (*G–J′*) MIST1 protein expression remains in adult *Gfi1*-null pancreas. MIST1 protein expression in adult WT and *Gfi1*-null mice (1 month old, 1M) was analyzed by immunofluorescence. The MIST1 protein expression pattern was comparable between WT (*G*, *G′*) and *Gfi1*-null pancreas (*H*, *H′*). However, BPL expression is noticeably disorganized in the *Gfi1*-null pancreas (*J*, *J′*) when compared with WT mice (*I*, *I′*). Scale bar: 50 μm.

Regardless of the outstanding question on CACs origin, it is significant that the *Gfi1* model provides evidence that there is a specific genetic function that helps create the terminal ductal structures of the organ and that this event happens well after the initial specification of the ductal lineage. The acinar/centroacinar unit has been referred to as a highly specialized compartment, having a fenestrated structure apical to the acinar cell that allows for effective draining of acinar zymogens. Regulation of pH appears to be important to immediately neutralize immature zymogen granule content should they enter this very restricted and limited space. Therefore, it perhaps is not unexpected that genetic mechanisms operate to secure proper development at this level, including the specification of a uniquely functioning cell—CAC—at the distal-most intercalated ductal network.

Mechanistically, the function of *Gfi1* in the pancreas is not understood. The *Gfi1* gene encodes a 55-kDa nuclear repressor, recruiting histone deacetylases to target promoters. At its C-terminus, it bears six typical C2H2-type zinc-finger domains that mediate sequence-specific DNA binding and the interaction with other proteins.[29] At its N-terminus, GFI1 has a 20-amino acid stretch that was named the SNAG (Snail/Gfi-1) domain because it is also found in the proteins Snail and Slug, which similarly have repressor functions.[29] Many interaction partners for GFI1 are known, mainly expressed within the hematopoietic system.[30] It is unclear whether these also represent pancreatic partners for GFI1, so it remains unknown which genomic regions are targeted by *Gfi1* in the pancreas as well. Among the possible *Gfi1*-repressed genes in the pancreas is *Ngn3*, as *Gfi1* and *Ngn3* are antagonistic in the gut; however, we did not observe an increase in endocrine cell formation at E14.5 in the *Gfi1*-null pancreas or obtain any evidence of endocrine cell differentiation at later stages or postnatally. We believe that due to the late-gestational phenotype, *Gfi1* repressor functions are more likely to be related to suppression of the gene-activation programs in the duct or acinar cells, allowing for their further specification. Mechanistic studies focused on *Gfi1* may provide new insight to the biology of the CACs.

It should be recognized that we cannot determine whether the lack of *Gfi1* leads to a complete block in the differentiation of CACs. It remains possible that such cells differentiate but lack expression of particular factors such as possibly HNF6, HNF1β, Sox9, which could be necessary for their structural program. In the absence of a specific intercalated ductal/CAC marker that would signify the presence of such a partially specified subpopulation, it is difficult to conclude that the cells are completely absent or present in another differentiated form. However, transmission electron microscopy imaging leads us to conclude that there are fewer cellular structures present in *Gfi1*-nulls at the apical exocrine position that are not provided by the exocrine cells themselves. We believe that the presence of structures provided by such dysfunctional intercalated ductal cells would be detected as a membrane lipid bilayer contribution proximal to the acinar cell if partially differentiated cells were present. Evidently, the acinar units in *Gfi1*-null mice were abnormal, and the loss of Claudin10 supported the notion that tight junctions at the apical position of the exocrine cells are defective in *Gfi1*-null pancreas.

In conclusion, we have reported on a novel gene in the pancreas, *Gfi1*, which serves a late role in organ development. These studies open a new window into understanding an elusive aspect of pancreatic biology—the formation of the CAC and the creation of a functional acinar unit. These studies also invite further exploration of the possible role of *Gfi1* in pancreatic disease and suggest a potential avenue for therapeutic intervention.

References

1. Gu G, Dubauskaite J, Melton DA. Direct evidence for the pancreatic lineage: NGN3+ cells are islet progenitors and are distinct from duct progenitors. Development 2002;129:2447–2457.
2. Cleveland MH, Sawyer JM, Afelik S, et al. Exocrine ontogenies: on the development of pancreatic acinar, ductal and centroacinar cells. Semin Cell Dev Biol 2012; 23:711–719.
3. Orci L, Ravazzola M, Anderson RG. The condensing vacuole of exocrine cells is more acidic than the mature secretory vesicle. Nature 1987;326:77–79.
4. Waterford SD, Kolodecik TR, Thrower EC, et al. Vacuolar ATPase regulates zymogen activation in pancreatic acini. J Biol Chem 2005;280:5430–5434.
5. Behrendorff N, Floetenmeyer M, Schwiening C, et al. Protons released during pancreatic acinar cell secretion acidify the lumen and contribute to pancreatitis in mice. Gastroenterology 2010;139:1711–1720.
6. Niederau C, Grendell JH. Intracellular vacuoles in experimental acute pancreatitis in rats and mice are an acidified compartment. J Clin Invest 1988;81:229–236.
7. Takacs T, Rosztoczy A, Maleth J, et al. Intraductal acidosis in acute biliary pancreatitis. Pancreatology 2013;13:333–335.
8. Shih HP, Wang A, Sander M. Pancreas organogenesis: from lineage determination to morphogenesis. Annu Rev Cell Dev Biol 2013;29:81–105.
9. Afelik S, Qu X, Hasrouni E, et al. Notch-mediated patterning and cell fate allocation of pancreatic progenitor cells. Development 2012;139:1744–1753.
10. Shih HP, Kopp JL, Sandhu M, et al. A Notch-dependent molecular circuitry initiates pancreatic endocrine and ductal cell differentiation. Development 2012;139: 2488–2499.
11. Afelik S, Jensen J. Notch signaling in pancreas: patterning and cell fate specification. WIREs Dev Biol 2013;2:531–544.
12. Pan FC, Wright C. Pancreas organogenesis: from bud to plexus to gland. Dev Dyn 2011;240:530–565.
13. Kopinke D, Brailsford M, Shea JE, et al. Lineage tracing reveals the dynamic contribution of Hes1+ cells to the developing and adult pancreas. Development 2011; 138:431–441.
14. Kopinke D, Brailsford M, Pan FC, et al. Ongoing Notch signaling maintains phenotypic fidelity in the adult exocrine pancreas. Dev Biol 2012;362:57–64.

15. Zhou ZC, Dong QG, Fu DL, et al. Characteristics of Notch2(+) pancreatic cancer stem-like cells and the relationship with centroacinar cells. Cell Biol Int 2013; 37:805–811.
16. Hock H, Orkin SH. Zinc-finger transcription factor Gfi-1: versatile regulator of lymphocytes, neutrophils and hematopoietic stem cells. Curr Opin Hematol 2006;13:1–6.
17. Linnoila RI, Jensen-Taubman S, Kazanjian A, et al. Loss of GFI1 impairs pulmonary neuroendocrine cell proliferation, but the neuroendocrine phenotype has limited impact on post-naphthalene airway repair. Lab Invest 2007;87:336–344.
18. Shroyer NF, Wallis D, Venken KJ, et al. *Gfi1* functions downstream of *Math1* to control intestinal secretory cell subtype allocation and differentiation. Genes Dev 2005; 19:2412–2417.
19. Wallis D, Hamblen M, Zhou Y, et al. The zinc finger transcription factor *Gfi1*, implicated in lymphomagenesis, is required for inner ear hair cell differentiation and survival. Development 2003;130:221–232.
20. Hock H, Hamblen MJ, Rooke HM, et al. Intrinsic requirement for zinc finger transcription factor Gfi-1 in neutrophil differentiation. Immunity 2003;18:109–120.
21. Qu X, Afelik S, Jensen JN, et al. Notch-mediated post-translational control of Ngn3 protein stability regulates pancreatic patterning and cell fate commitment. Dev Biol 2013;376:1–12.
22. Hashizume A, Ueno T, Furuse M, et al. Expression patterns of claudin family of tight junction membrane proteins in developing mouse submandibular gland. Dev Dyn 2004;231:425–431.
23. Sengupta A, Valdramidou D, Huntley S, et al. Distribution of MUC1 in the normal human oral cavity is localized to the ducts of minor salivary glands. Arch Oral Biol 2001; 46:529–538.
24. Jensen JN, Cameron E, Garay MV, et al. Recapitulation of elements of embryonic development in adult mouse pancreatic regeneration. Gastroenterology 2005; 128:728–741.
25. Siveke JT, Lubeseder-Martellato C, Lee M, et al. Notch signaling is required for exocrine regeneration after acute pancreatitis. Gastroenterology 2008;134: 544–555.
26. Heremans Y, Van De Casteele M, in't Veld P, et al. Recapitulation of embryonic neuroendocrine differentiation in adult human pancreatic duct cells expressing neurogenin 3. J Cell Biol 2002;159:303–312.
27. Kopp JL, Dubois CL, Schaffer AE, et al. Sox9+ ductal cells are multipotent progenitors throughout development but do not produce new endocrine cells in the normal or injured adult pancreas. Development 2011; 138:653–665.
28. Phelan JD, Saba I, Zeng H, et al. Growth factor independent-1 maintains Notch1-dependent transcriptional programming of lymphoid precursors. PLoS Genet 2013;9:e1003713.
29. Chiang C, Ayyanathan K. Snail/Gfi-1 (SNAG) family zinc finger proteins in transcription regulation, chromatin dynamics, cell signaling, development, and disease. Cytokine Growth Factor Rev 2013;24:123–131.
30. Phelan JD, Shroyer NF, Cook T, et al. *Gfi1*-cells and circuits: unraveling transcriptional networks of development and disease. Curr Opin Hematol 2010;17: 300–307.

Received August 6, 2014. Accepted December 5, 2014.

Correspondence
Address correspondence to: Jan Jensen, PhD, Department of Stem Cell Biology and Regenerative Medicine, Lerner Research Institute, Cleveland Clinic Foundation, 9500 Euclid Avenue, Cleveland, Ohio 44195. e-mail: jensenj2@ccf.org.

Acknowledgments
The authors thank multiple investigators for donating antibodies, and S. Afelik and M. Bukys for their critical reading of the manuscript.

Conflicts of interest
The authors disclose no conflicts.

Funding
This study was funded by a graduate stipend from the University of Copenhagen (to P.N.); and the American Diabetes Association (1-11-BS-75), the National Institutes of Diabetes and Digestive and Kidney Diseases (Grant 1R01-DK097087), the Cleveland Clinic Foundation, and a gift from the E. J. Brandon family (to J.J.). This work was also supported by the Chicago Diabetes Project (www.thechicagodiabetesproject.org).

Supplementary Table 1. Information about Primary Antibodies and Lectin Dye

Antibody	Species	Source	Product ID	Lot No.	Dilution
Anti-amylase	Rabbit	Sigma-Aldrich, St. Louis, MO	A8273	077h9044	1:500
Anti-ghrelin	Goat	Santa Cruz Biotechnology, Santa Cruz, CA	SC10368	F0105	1:200
Anti-chrom A	Rabbit	Abcam, Cambridge, MA	ab17064	GR192521-1	1:250
Anti-glucagon	Mouse	Sigma-Aldrich	ab10988	G2654	1:100
Anti-insulin	Guinea pig	Novo-Nordisk, Bagsvaerd, Denmark	A0564	10057850	1:500
Anti-Pdx1	Goat	Dr. C.V. Wright, Nashville, TN	—	—	1:2000
Anti-Sox9	Rabbit	Millipore, Billerica, MA	AB5535	2167153	1:2000
Anti-HNF6	Rabbit	Santa Cruz Biotechnology	sc-13050	C0310	1:50 (TSA)
Anti-pHH3	Rabbit	Millipore	06-570	2066052	1:200
Anti-mucin 1	Hamster	NeoMarkers, Fremont, CA	HM-1630-P	1630P805A	1:200
Anti-BrdU	Mouse	BD Biosciences, San Jose, CA	347580	56065	1:100
Anti-CPA1	Mouse	Abcam	ab84999	GR107104-1	1:200
Anti-claudin10	Rabbit	Abcam	ab24792-100	455776	1:200
Anti-HNF1β	Rabbit	Santa Cruz Biotechnology	sc-22840	I0205	1:100
Anti-E-cadherin	Rat	Invitrogen, Frederick, MD	131900	73650155	1:200
Fluorescein-Bauhenia	Purpurea lectin	Vector Labs, Burlingame, CA	FL-1281	Q0910	1:100
Fluorescein-Dolichos	Biflorus agglutinin	Vector Labs	FL-1031	W1130	1:100

TSA, tyramide-stimulated amplification.